Proceedings of the
10th Graz Brain-Computer Interface Conference 2026

10.3217/978-3-99161-093-9-035

Non-invasive measurement of somatosensory evoked spinal cord potentials

Bernhard Golser[1], Markus Oberndorfer[1], Kyriaki Kostoglou[1], Gernot R. Müller-Putz [1,2]

[1]Institute of Neural Engineering, Graz Brain-Spine Lab, Graz University of Technology, Graz, Austria
[2]BioTechMed Graz, Graz, Austria

E-mail: gernot.mueller@tugraz.at

ABSTRACT: The spinal cord is more than a mere relay station between the brain and the peripheral nervous system. Recent research indicates that complex processing already occurs at the spinal level. The non-invasive recording of spinal cord activity acquired with high-density surface electrode arrays may advance our understanding of spinal network dynamics and the integration of spinal data could enhance existing brain–computer interfaces. In the present study, electroencephalography and electrospinography were used to measure cortical and spinal somatosensory evoked potentials elicited by median and tibial nerve stimulation in 10 healthy individuals. In contrast to previous studies, participants were seated upright with no external support of the head and stimulus intensities were kept strictly below the movement threshold. Under these more physiologically realistic settings, two of the three well-characterized spinal cord components (N13 and P22) were successfully detected, indicating a broader variety of potentially successful experimental setups.

INTRODUCTION

Being the most caudal part of the central nervous system (CNS), the spinal cord links the peripheral nervous system (PNS) to the brain. Several studies have shown that complex processing already occurs at the spinal level, contributing to both motor and somatosensory functions [1] [2]. Capturing this spinal activity non-invasively is possible using surface electrodes and is referred to as the electrospinogram (ESG). However, compared to the electroencephalogram (EEG) the ESG has received considerably less attention in scientific research. This may be, in part, due to the technical challenges associated with recording the ESG. Small signal amplitudes and large artifactual sources such as electric activity from the heart and surrounding muscles complicate its measurement. Existing research mainly focuses on the somatosensory evoked spinal cord potential (SCP), since its phase-locked nature facilitates signal enhancement by averaging across multiple trials [3] [4] [5] [6]. These potentials reflect activity along the somatosensory pathway. Afferent potentials traveling along this pathway pass through at least three neurons: primary afferents of the PNS are pseudounipolar neurons located in the dorsal root ganglion. Their dendrites pick up signals generated by various sensory receptors, which are consequently relayed to the CNS via the neurons' axons. They enter the spinal cord through the dorsal roots and project to neurons in the CNS. These secondary afferent neurons are located in the dorsal horn, the medulla oblongata or the pons and in turn project to the thalamus. Subsequently, the signals are relayed to the somatosensory cortex by tertiary afferent neurons [7]. The so-called segmental SCP is evoked by stimulation of a peripheral nerve or a dorsal root and is recorded at the corresponding spinal segment [8]. It is composed of three main peaks characterized by their latency in ms. The first, positive peak (P9) represents afferent volleys traveling towards the dorsal root and entering the spinal cord [8]. Others have argued that P9 could reflect far field potentials stemming from afferent volleys in the brachial plexus [3]. The second, negative peak (N13) represents activity of secondary afferents and interneurons within the spinal segments targeted by stimulation [8]. The final well defined characteristic of the SCP is a slow, positive wave termed P22. Just as the two preceding components it is also detectable in the spinal segment corresponding to the stimulation site. It has been hypothesized that it reflects presynaptic inhibition by primary afferent depolarization [5] [8]. Although measurements conducted using epidural electrodes or needle electrodes yield a higher signal quality, the aforementioned SCP components have also been detected in surface electrode recordings, demonstrating the feasibility of non-invasive ESG recordings [6] [9] [10]. However, previous studies employed mixed nerve stimulation above the motor threshold, which yields higher SCP amplitudes, but is not representative of physiological somatosensory stimuli such as touch or pain. Additionally, previous studies minimized electromyogram (EMG) contamination by recording participants in supine or reclined positions that promote relaxation of neck muscles. While such conditions enhance the signal-to-noise ratio, they restrict the range of possible experimental approaches. In the present study, we aim to address these limitations by recording cervical SCPs following median nerve stimulation (MNS) at a stimulation intensity strictly below the motor threshold to avoid the recording of movement-related components. Recordings are obtained with participants seated in an upright position,

10.3217/978-3-99161-093-9-035

forcing them to engage the stabilizing muscles in their neck. Comparative measurements in response to tibial nerve stimulation (TNS) are conducted to validate the neurogenic nature of SCPs following MNS. We hypothesize that MNS will elicit the previously described waveform, whereas TNS will not produce cervical responses at the corresponding latencies, since the spinal segments associated with the tibial nerve are located further caudally. Concurrent cortical somatosensory evoked potentials (SEPs) are recorded to confirm successful stimulation. Importantly, we introduce a novel and reproducible electrode placement system for cervical ESG recordings based on easily identifiable anatomical landmarks, providing a standardized framework for future non-invasive spinal measurements.

MATERIALS AND METHODS

Participants: Ten able-bodied students participated in the study (three female). The mean age was 26.6 years (range: 25–30 years). Participants received financial compensation for their participation.

Paradigm: All recordings were conducted in a quiet, electromagnetically shielded room at a pleasant temperature. The participants were seated in a comfortable chair and were asked to adopt a relaxed position. During recordings they were asked to sit still and keep their gaze focused on a fixed point, but were specifically instructed to adjust their seating position any time they felt uncomfortable and to breath and blink normally. These instructions were given to prevent excessive EMG contamination due to a tense posture.
Two stimulation conditions were defined according to the major nerves targeted: MNS of the upper and TNS of the lower extremity. A total of 4000 stimulations were delivered per participant and condition, amounting to 8000 stimulations per session. The inter-stimulus-interval was sampled from a uniform distribution ranging from 700 to 900 ms. To minimize discomfort, the recordings were split into ten runs (five for each condition) of 800 stimulations, each run lasting approximately 11 minutes. MNS and TNS runs were executed in random order to avoid biases due to fatigue or habituation. Prior to the stimulation runs, 14 minutes of data for the resting state condition were recorded. Including breaks, the total recording time amounted to approximately three hours.

Stimulation setup: Electrical stimulation was delivered using the *Digitimer DS7R Constant Current Stimulator* (Digitimer, Letchworth Garden City, UK) and a pair of *Flextrode Plus 32mm* surface electrodes (Krauth+Timmermann, Hamburg, Germany). The device was set to monophasic stimulation with a pulse duration of 200 μs. In all participants, stimulations were delivered to the right side of the body for both MNS and TNS with stimulation currents strictly below the motor threshold to avoid motor components in the recorded signal. To minimize artifacts caused by the stimulation current, a ground-clamp was attached proximal to the respective

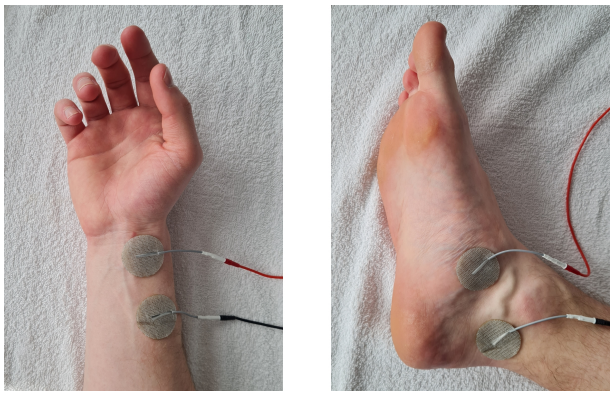

Figure 1: **Stimulation setup.** Approximate location of the stimulation electrodes for MNS (left) and TNS (right).

stimulation site. For MNS, the stimulation electrodes were placed on the radial side of the forearm, with the anode just proximal to the wrist. The cathode was placed proximal to the anode. The exact electrode positions were determined by trial and error: after an initial positioning, a stimulus above the motor threshold was delivered and the motor response was observed. The electrode positions were re-adjusted until the stimulus led to a twitch of the thumb, indicating a correct stimulation of the median nerve [11]. Once the electrode positions were established, the motor threshold was determined by gradually reducing the stimulation current until no motor response was visible. One participant did not tolerate stimulation currents high enough to trigger a motor response. In this case, the highest bearable stimulation current was applied and the electrode positions were determined based on the experience gained with previous participants. The same procedure was followed for TNS. The electrodes were placed on the medial side of the participant's ankle. The exact positions were once again determined by applying a stimulus above the motor threshold and observing the motor response. A plantar flexion of the first toe indicated the correct position [11]. Figure 1 shows the approximate electrode sites for MNS and TNS.

EEG recording: Both EEG and ESG were recorded using active electrodes and the *BrainAmp Standard* amplifier (Brain Products, Gilching, Germany). The amplifier's internal highpass filter and lowpass filter were set to 1 Hz and 1000 Hz, respectively. Signals were acquired with a sampling rate of 5000 Hz. The EEG was recorded using 28 electrodes. The electrode montage followed the standard 10-10 system, using the following electrode positions: *FC5, FC3, FC1, FCZ, FC2, FC4, FC6, C5, C3, C1, Cz, C2, C4, C6, CP5, CP3, CP1 CPZ, CP2, CP4, CP6, P5, P3, P1, Pz, P2, P4, P6*. Additionally, electrodes were placed on the left and right mastoids for later re-referencing. The ground electrode was placed on the forehead while the reference electrode was placed on the tip of the nose to provide a symmetric reference.

ESG electrode system: In the course of this study, a reproducible electrode system for high-density ESG recordings was developed. Derived from the well-established 10-10 system for EEG measurements, it uti-

10.3217/978-3-99161-093-9-035

lizes visible or palpable landmarks to define anatomically sensible positions for 54 electrodes. The vertical inter-electrode distance is defined as one fifth of the distance between the spinous process of the second cervical vertebra and the spinous process of the seventh cervical vertebra. Similarly, the horizontal inter-electrode distance is defined as one fifth of the distance between the left and right spinous process of the first cervical vertebra. Figure 2 displays the mentioned reference points and distances and the full ESG electrode layout. The ESG nomenclature was defined according to the following system: the first letter, *S* for *spine*, clearly distinguishes the ESG from the EEG nomenclature. It is followed by a number to determine the electrode's horizontal position. As in EEG nomenclature, uneven numbers are used for the left and even numbers for the right side, with higher numbers indicating a more lateral position. The number is followed by a *C* for *cervical* or a *T* for *thoracic*. The final number indicates the approximate vertical level of the electrode with respect to the closest spinous process. The active electrodes were attached to the participant's neck with adhesive rings. To ensure precise placement, the necessary distances were measured and markings were made on the participant's skin. The skin of the neck was thoroughly cleansed with alcohol prior to attaching the electrodes. Electrode gel was applied and allowed to settle in order to reduce impedance. As with the EEG electrodes, the ESG electrodes were also referenced to the nose-electrode. EEG and ESG recordings as well as triggers were synchronized via Lab Streaming Layer [12].

Processing: Signal processing was performed in *Matlab R2023b* [13]. Prior to any further processing, all recording sessions were visually inspected. Channels that were corrupted throughout an entire run were excluded from the respective session. Subsequently, short sections contaminated by large EMG artifacts (e.g., due to participants adjusting their sitting posture) were removed manually. The resulting dataset was re-referenced to the left and right mastoids' average potential. Power-line interference at 50 Hz and its harmonics were removed using a comb filter. Additionally, a 4$^{\text{th}}$ order butterworth highpass filter at 0.5 Hz was applied. To remove artifactual signal components such as the electrocardiogram (ECG) from the data, independent component analysis (ICA) was employed using the function *runica* implemented in *EEGLAB* [14]. To improve ICA decomposition while preserving high-frequency components, the ICA weights were computed on data band-pass filtered between 1 and 60 Hz. These weights were subsequently applied to the unfiltered dataset, and the resulting independent components (ICs) were visually inspected for rejection. Topographical maps were generated for each IC to assist classification. Subsequently, MNS and TNS data were epoched relative to the stimulus onset, whereas resting state data were segmented into non-overlapping epochs. Approximately 5-10% of epochs of each participant were rejected based on amplitude thresholding, their joint probability and their kurtosis [14]. All epochs

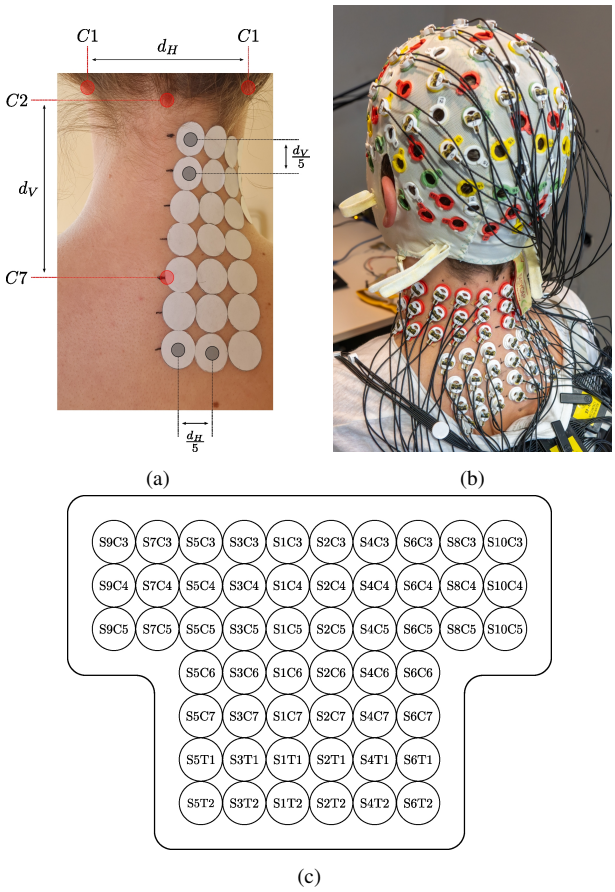

Figure 2: **ESG electrode system and measurement setup.** **a)** Explanation of the ESG electrode system. *C*2 and *C*7 mark the locations of the respective spinous processes as determined by palpation. The labels *C*1 indicate the transverse processes of the first cervical vertebra. d_V is the vertical distance between *C*2 and *C*7 while d_H is defined as the horizontal distance between the transverse processes of *C*1. The vertical and horizontal inter-electrode distances are defined by $\frac{d_V}{5}$ and $\frac{d_H}{5}$, respectively. **b)** Full EEG and ESG electrode setup. **c)** ESG electrode layout and nomenclature. The letter S stands for spine, distinguishing ESG from EEG electrodes. It is followed by a number to determine the electrode's horizontal position. Uneven numbers are used for the left and even numbers for the right side, with higher numbers indicating a more lateral position. This is followed by a combination of the letter *C* or *T* (for *cervical* or *thoracic*) and a number, indicating the approximate vertical level of the electrode with respect to the closest spinous process.

were baseline corrected with respect to the interval −55 to −5 ms. Subsequently, grand averages were calculated. For visualization purposes, 95% confidence intervals were calculated for each condition and displayed as shaded areas around the average time courses. Local extrema around the expected latencies of N13 (t = 12.4 ms) and P22 (t = 22.2 ms) could be identified. The MNS and TNS conditions were tested against the rest condition at these latencies using linear mixed-effect models with the condition as a fixed effect and the participant as a random intercept to account for repeated measurements within participants. Benjamini–Hochberg correction was applied to account for multiple comparisons [15]. ESG

10.3217/978-3-99161-093-9-035

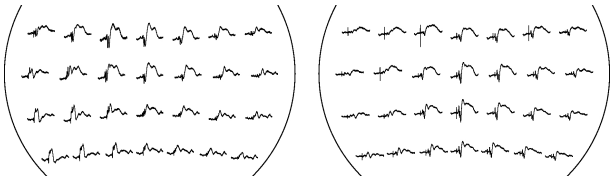

Figure 3: **Cortical somatosensory evoked potentials.** SEPs recorded in response to MNS (left) and TNS (right) displayed at their respective locations on the scalp. The traces are plotted in the time range -120 to 430 ms with respect to the stimulation onset for both conditions.

topoplots at the tested latencies were created by spline interpolation between the individual electrode sites.

RESULTS

Cortical somatosensory evoked potentials: EEG measurements were performed, in part, to validate the effective stimulation of the median and tibial nerve. Figure 3 illustrates the SEPs recorded across the scalp. The contralateral nature of the evoked potentials following MNS was clearly visible, while the response to TNS was more central with a slight tendency towards the ipsilateral (right) side in the later components.

Somatosensory evoked spinal cord potentials: At the group level, two of the three major peaks described in literature could be identified in our SCP recordings. Figure 4 displays evoked waveforms and their corresponding topographical distributions following MNS and TNS. At a latency corresponding to N13, four electrodes, most of them located rather rostral and medial, showed significant amplitudes after MNS compared to rest (see Subfigure 4a). No clear lateralisation was visible and the wave had a duration of approximately 5 ms. The comparison to TNS served as a control condition. No significant amplitudes were visible at this latency in response to TNS, which had been expected. The peak at a latency associated with P22 covered a much larger area of the neck, with its maximum intensity in the rostral area on the ipsilateral (right) side (Subfigure 4b). A region of reduced amplitudes was distinguishable in the ipsilateral, caudal part of the electrode grid. With a duration of approximately 20 ms, this wave was much broader than the previously described N13. Again, TNS did not lead to any significant activity at the latency of interest.

Somatosensory pathway: Figure 5 depicts the potentials evoked by MNS recorded along the somatosensory pathway in this study, all of which have been previously described in literature [8] [16]. The figure clearly shows that the earliest component registered in this study was a negative peak that appeared over the cervical spinal cord (N13), which is attributed to postsynaptic activity in the dorsal horn [8]. N13 was followed by far field potentials measured on the scalp representing activity in the area of the cuneate nuclues and the medial lemniscus (P14) [17]. Subsequently, a more localized potential registered above the contralateral somatosensory areas indicated the afferent signal's arrival at the cortex (N20). Finally, P22 represented subsequent activity at the spinal level, ascribed to primary afferent depolarisation and top-down feedback from supraspinal structures [8] [18].

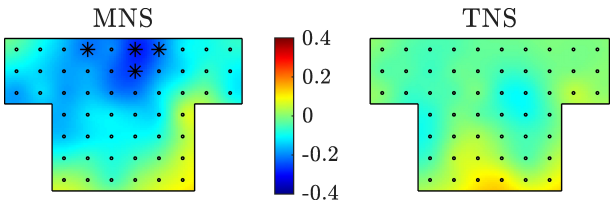

(a) Topographic maps at a latency of 12.4 ms after MNS and TNS

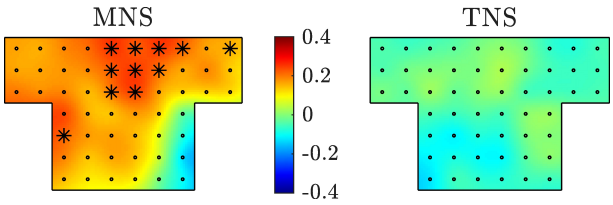

(b) Topographic maps at a latency of 22.2 ms after MNS and TNS

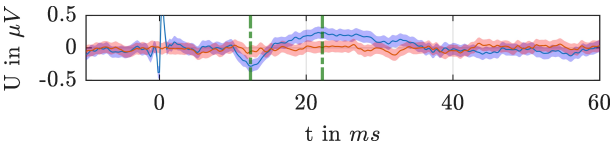

(c) Grand average time course of S2C3 after MNS

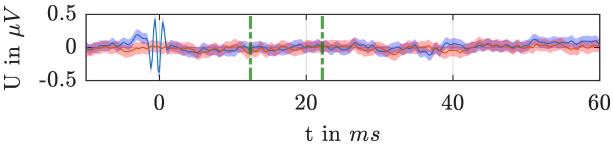

(d) Grand average time course of S2C3 after TNS

Figure 4: **SCPs after MNS and TNS.** The topographic maps on the left in **a)** and **b)** display the signal distribution after MNS at the maximum of N13 and P22, respectively. Electrodes marked with an asterisk showed significant activity compared to rest at the corresponding latency. Note the central and rostral location of N13 and the broader area affected by P22. The topographic plots on the right in **a)** and **b)** display the signal distribution at the same latencies after TNS. Note that no significant activity compared to rest was captured at these latencies as a result of TNS. **c)** Grand average SCP elicited by MNS in one representative electrode. **d)** Signal captured in the same electrode in response to TNS. The blue traces represent the signal recorded after MNS (**c**) and TNS (**d**), the red trace represents the rest condition. The dashed vertical lines mark the latencies of N13 and P22. Shaded areas indicate the 95% confidence interval.

DISCUSSION

Cortical somatosensory evoked potentials: In general, the grand average SEPs recorded after both MNS and TNS were consistent with existing literature. As expected, the topographic plots showed a lateralization towards the contralateral side with respect to the stimulated side in case of MNS, which reflects the location of the respective areas within the somatosensory cortex [16]. The evoked potentials following TNS were localized above the center of the somatosensory cortex and

10.3217/978-3-99161-093-9-035

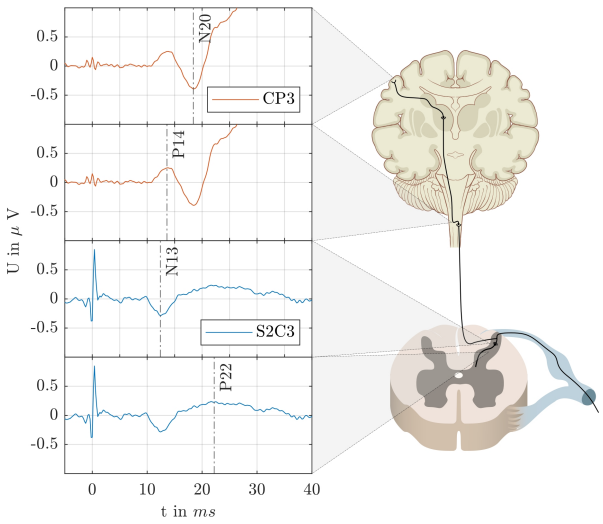

Figure 5: **Responses to MNS along the somatosensory pathway recorded in this study.** The peaks marked in the traces of SEP and SCP on the left hand side of the figure are allocated to their respective regions of origin in the sketch on the right. The blue traces in the two bottommost plots are SCPs recorded in the ESG electrode S2C3, showing the peaks N13 and P22. The upper two orange traces are SEPs recorded in CP3, reflecting P14 and N20. Sketches adapted from [19] [20].

showed a deviation to the ipsilateral side. This deviation is unexpected and could not be explained. One reason for recording the EEG response was to validate MNS and TNS. Considering the grand average traces and the fact, that SEPs were evoked in all participants at the individual level, it can be concluded that both median and tibial nerve stimulation were successful.

Somatosensory evoked spinal cord potentials: At the group level, the evoked SCP was clearly visible. Although the precise anatomical origins of the individual components cannot be determined from surface electrode recordings, the observed waveforms were consistent with descriptions reported in literature [6] [8] [18] [21] [22] [23]. As previously described, N13 and P22 were both observable in our data. Interestingly, both potentials were recorded at quite rostral levels, with N13 being maximal at the level of the spinous processes C3 and C4. Considering that the median nerve projects to the spinal segments Th1 to C6 this is unexpected. Similarly rostral locations of N13 have been reported previously [4] [22]. Part of this upward shift might be explained by the spine's anatomy: the processes used to estimate the location of the corresponding spinal segments protrude in caudal direction. Additionally, the respective spinal segment is situated above the corresponding vertebra. As a result, the electrode row ascribed to a certain spinal segment was probably placed too far caudally with respect to this segment. This at least partly explains why N13 was recorded so far rostrally. However, since shape and timing of the recorded peaks are in line with literature, it can be concluded that we successfully recorded N13 (reflecting postsynaptic activity in the dorsal horn) and P22 (reflecting activity resulting from top-down feedback or primary afferent depolarisation). However, P9 was not apparent in our data. The observation that N13 and P22 were detectable whereas P9 was not may be attributed to the postsynaptic origin of N13 and P22. P9 reflects afferent volleys and the strength of these volleys is related to the amount of nerve fibres recruited by stimulation. Small stimuli result in a low number of recruited fibres [24], which in turn results in small signal amplitudes when recording summed potentials of said volleys using surface electrodes. However, N13 is caused by the activity of a network of neurons that receives input from these primary afferents. Coombs et al. [25] proposed that repetitive firing within this network might cause the prolonged duration of the N13 peak. It is plausible that such sustained postsynaptic activity facilitates the detectability of N13 in our setup. A similar argument may explain the detectablility of P22. Even though the afferent volleys elicited by sub-threshold stimulation may have been too weak to produce a measurable P9 component, they were sufficient to evoke robust cortical responses. The resulting top-down feedback hypothesized to underlie P22 likely generated sufficient activity within the corresponding spinal segment to permit non-invasive recording.
Taken together, our findings demonstrate that cervical somatosensory evoked SCPs can be recorded non-invasively using a high-density surface electrode array. To our knowledge, this is the first report of cervical SCPs obtained with sub-motor-threshold MNS in participants seated upright without head support. Despite these less optimized conditions, the components N13 and P22 were reliably detectable at the group level, whereas the component P9 was not observed. Achieving statistically significant effects under these conditions required a substantially larger number of stimuli compared to studies employing higher stimulation intensities or supine recordings. Nevertheless, these results extend previous work and indicate that non-invasive ESG recordings remain feasible in more naturalistic experimental settings. Recent advances in spinal electrophysiology, including single-trial SCP detection using spatial filtering techniques [23], reports of attentional modulation of P22 [18] and the proposal of an alternative ESG electrode layout [22], highlight a rekindled interest in non-invasive assessment of spinal processing. In this context, the present dataset provides a valuable basis for future research, such as the analysis of spino-cortical connectivity.

Limitations: Despite these promising findings, several limitations should be considered. The proposed electrode layout is reproducible and anatomically sensible. However, the anatomical relationship between spinal segments and their corresponding vertebra does not hold for more caudal regions of the spinal column. Hence, adjustments would be necessary for thoracic and lumbar measurements. Regarding signal processing, the manual removal of ECG via ICA was successful but time-consuming. Other promising methods for ECG removal

10.3217/978-3-99161-093-9-035

have been proposed [22] [23].

CONCLUSION

Our findings demonstrate the feasibility of non-invasively recording somatosensory evoked spinal cord potentials under more naturalistic conditions, suggesting a broader range of viable paradigms. In light of the renewed interest in non-invasive spinal recordings across several groups, such approaches may play an important role in advancing our understanding of spinal-level processing. Furthermore, incorporating spinal signals into existing BCI approaches may provide a missing link with the potential to enhance system performance in the future.

REFERENCES

[1] Chirila AM et al. Mechanoreceptor signal convergence and transformation in the dorsal horn flexibly shape a diversity of outputs to the brain. Cell. 2022;185(24):4541–4559.e23.
[2] Lorach H et al. Walking naturally after spinal cord injury using a brain-spine interface. Nature. 2023;618(7963):126–133.
[3] Desmedt JE, Nguyen TH. Bit-mapped colour imaging of the potential fields of propagated and segmental subcortical components of somatosensory evoked potentials in man. Electroencephalography and clinical neurophysiology. 1984;58(6):481–497.
[4] Hallström YT, Lindblom U, Meyerson BA, Prevec TS. Epidurally recorded cervical spinal activity evoked by electrical and mechanical stimulation in pain patients. Electroencephalography and clinical neurophysiology. 1989;74(3):175–185.
[5] Jeanmonod D, Sindou M, Mauguière F. The human cervical and lumbo-sacral evoked electrospinogram. data from intra-operative spinal cord surface recordings. Electroencephalography and clinical neurophysiology. 1991;80(6):477–489.
[6] Shimoji K, Shimizu H, Maruyama Y. Origin of somatosensory evoked responses recorded from the cervical skin surface. Journal of neurosurgery. 1978;48(6):980–984.
[7] Waldeyer A, Anderhuber F, Pera F, Streicher J. Waldeyer - anatomie des menschen. DE GRUYTER (2012).
[8] Kano T, Katayama Y, Fukuda S, Shimoji K, Willis WD. Evoked spinal cord potentials. Springer Japan: Tokyo (2006).
[9] Di Lionardo A et al. Modulation of the n13 component of the somatosensory evoked potentials in an experimental model of central sensitization in humans. Scientific reports. 2021;11(1):20838.
[10] Di Pietro G et al. The n13 spinal component of somatosensory evoked potentials is modulated by heterotopic noxious conditioning stimulation suggesting an involvement of spinal wide dynamic range neurons. Neurophysiologie clinique = Clinical neurophysiology. 2021;51(6):517–523.
[11] Mauguière F et al. Somatosensory evoked potentials. the international federation of clinical neurophysiology. Electroencephalography and clinical neurophysiology. Supplement. 1999;52:79–90.
[12] Kothe C et al. The lab streaming layer for synchronized multimodal recording. Imaging neuroscience (Cambridge, Mass.). 2025;3.
[13] Inc. TM. *Matlab version: 9.13.0 (r2023b)*. Natick, Massachusetts, United States, 2023. [Online]. Available: https://www.mathworks.com
[14] Delorme A, Makeig S. Eeglab: An open source toolbox for analysis of single-trial eeg dynamics including independent component analysis. Journal of neuroscience methods. 2004;134(1):9–21.
[15] Benjamini Y, Hochberg Y. Controlling the false discovery rate: A practical and powerful approach to multiple testing. Journal of the Royal Statistical Society Series B: Statistical Methodology. 1995;57(1):289–300.
[16] Stöhr M. Evozierte potenziale: Sep - vep - aep - ekp - mep. Springer Medizin Verlag Heidelberg: Berlin, Heidelberg (2005).
[17] Eisen A. The somatosensory evoked potential. The Canadian journal of neurological sciences. Le journal canadien des sciences neurologiques. 1982;9(2):65–77.
[18] Gabrieli G, Somervail R, Mouraux A, Leandri M, Haggard P, Iannetti GD. Electrical spinal imaging: A noninvasive, high-resolution approach that enables electrophysiological mapping of the human spinal cord. PLoS biology. 2025;23(11):e3003116.
[19] Aguayo M. Imgnotraçat arc refelx. [Online; accessed April 8, 2025]. 2014. [Online]. Available: https://commons.wikimedia.org/wiki/File:Imgnotra%C3%A7at_arc_refelx_esp.svg
[20] Lynch PJ, Jaffe CC. Human brain coronal section. [Online; accessed April 8, 2025]. 2006. [Online]. Available: https://commons.wikimedia.org/wiki/File:Brain_human_coronal_section.svg
[21] Cracco RQ. Spinal evoked response: Peripheral nerve stimulation in man. Electroencephalography and clinical neurophysiology. 1973;35(4):379–386.
[22] Mehra P et al. Sc10x/u: A high-density electrode system for standardised surface recording of neural activity of the cervical spinal cord. Clinical Neurophysiology. 2025;177:2110824.
[23] Nierula B et al. A multichannel electrophysiological approach to noninvasively and precisely record human spinal cord activity. PLOS Biology. 2024;22(10):1–41.
[24] Müller-Putz G, Rupp R. Neuroprosthetics and brain-computer interfaces in spinal cord injury. Springer International Publishing: Cham (2021).
[25] Coombs JS, Curtis DR, Landgren S. Spinal cord potentials generated by impulses in muscle and cutaneous afferent fibres. 1956;19(5):452–467.